### Cume 396

The paper is about the structure of the dwarf irregular galaxy NGC1569. Table 1 provides a list of key parameters of this galaxy such as the stellar and HI gas mass, rotational velocity  $V_{\rm rot}$  and maximum circular velocity  $V_{\rm max}$ . Figures 15 and 17 give plots of velocity curves and compare results with the cosmological Navarro-Frenk-White (NFW) profile. The passing grade for this cume is 70%.

- (1) 15pt The text says that the stars in NGC1569 are in a thick disk with a  $V_{\text{max}}/\sigma_z = 2.4$ . However, this is a relative measure because it is a ratio of velocities. More detailed results (disk scale length and scale height) are given in Table 1. Please, compare  $V_{\text{max}}/\sigma_z$ , the disk scale length and scale height with those of our Milky Way galaxy. Which galaxy is thicker/thinner, hotter/colder in relative and absolute values?
  - For our Milky Way  $V_{\text{max}} = 230 \,\text{km/s}$ ,  $R_{\text{disk}} = 3 \,\text{kpc}$ ,  $z_0 = 0.3 \,\text{kpc}$ , and  $\sigma_z = 20 \,\text{km/s}$ . So, the stellar disk of or Galaxy has the same absolute thickness and rms velocity in z-direction as the dwarf galaxy. However, in relative units MW disk is thinner and colder  $(V_{\text{max}}/\sigma_z = 11)$ .
- (2) 20pt The maximum circular velocity  $V_{\text{max}} = 50 \,\text{km/s}$  (Table 1) is larger than the maximum rotational gas velocity  $V_{\text{rot}} = 33 \,\text{km/s}$  (Table 1 and Figure 15). Explain the reason for the difference between the circular velocity and rotational velocity. Why is the circular velocity larger than the rotational velocity? In order to estimate the difference, you need to write the balance of relevant forces including the centrigual force.
  - The difference between the circular and rotational velocities is called "asymmetric drift", which is related with random velocities. In equilibrium all forces (including centrifugal due to rotation) should sum up to zero:

$$\frac{V_{rot}^2}{R} = \frac{1}{\rho} \frac{dP}{dR} + \frac{GM(R)}{R^2},\tag{1}$$

where R is the distance to galaxy center, and P is either the gas pressure or the pressure of random velocities  $P = \rho \sigma^2$ . The circular velocity by definition is  $V_{circ} = \sqrt{GM/R}$ . Use it to find the relation between the circular velocity and rotational velocity:

$$V_{rot}^2 = V_{circ}^2 + \frac{R}{\rho} \frac{dP}{dR}.$$
 (2)

Because for any realistic system the pressure (or random velocities) decline with increasing distance,  $V_{rot} < V_{circ}$ . The pressure gradient (and thus, the asymmetric drift correction) can be found by measuring the surface density of HI and assuming that it has a constant height.

- (3) 15pt Using Figure 17, estimate the dynamical mass, the mass of dark matter, and the ratio of mass of baryons to the mass of dark matter inside the 2.5 kpc sphere centered on the galaxy. Note that the NFW profile on the plot should be ignored for this problem because it is from halo abundance matching, not from mass modeling.
  - At radius 2.5 kpc Figure 17 gives the circular velocity  $V_{circ} = 50 \,\mathrm{km/s}$  and contributions of gas and stars:  $V_{circ,gas} = V_{circ,stars} = 20 \,\mathrm{km/s}$ . The dynamical mass (the sum of all components including the dark matter) is

$$M_{dyn} = \frac{RV_{circ}^2}{G} = (50 \times 10^5)^2 \cdot 2.5 \cdot kpc/(GM_{\odot}) = 1.44 \times 10^9 M_{\odot}.$$
 (3)

Subtracting the contributions of gas and stars, we get mass of the dark matter:

$$M_{dm} = 9.8 \times 10^8 M_{\odot}.$$
 (4)

This gives the fraction of baryons  $M_{bar}/M_{dm} = 0.47$ . Note that the cosmological fraction of baryons is about 0.17. So, the galaxy has a remarkably large fraction of baryons for a dwarf galaxy.

- (4) 15pt The abstract says that the expected virial mass determined from halo abundance matching agrees with the observed mass profile at 2.2 kpc. Explain the halo abundance matching method. What observational and theoretical quantities does one need to know to apply the method?
  - The halo abundance matching (HAM) assumes that the main factor that defines the luminosity of a galaxy is the virial mass of its dark matter halo. Thus, more massive galaxies should be hosted by more massive halos. In order to apply the method we need to know the stellar luminosity function and the halo mass function. Using the galaxy luminosity function, we can find how many galaxies with different luminosities should be observed in some large volume of space. For the same volume we can find the number of halos with different masses. After ranking halos by mass and galaxies by luminosity, we start assigning the most luminous galaxy to the mass massive halo, the second luminous galaxy to the second massive halo and so on. At the end of the process every galaxy has dark matter mass.
- (5) 15pt The paper uses the tilted ring model to find the rotation curve of HI gas in the galaxy. Explain what the tilted ring model is.
- (6) 20pt In order to find the total gas mass, the authors corrected the HI mass to account for helium. How would you do this? Should we also add a correction for other elements? How large a correction do you expect?
  - Helium abundance (by mass) is about 25 percent. It slightly depends on the overall metallicity in the galaxy. We can add about 2% for other elements, but the main contribution comes

from helium. If  $n_{He}$  and  $n_{H}$  are the densities of helium and hydrogen, then 25% of helium means that

$$\frac{4n_{He}}{4n_{He} + n_H} = 0.25. ag{5}$$

Correction factor to account for helium is  $(4n_{He} + n_H)/n_H = 1.33$ . Slightly more accurate estimate used in the paper is the factor 1.37. This is due to a larger abundance of helium and  $\sim 2\%$  of other elements.

$$G = 6.674 \times 10^{-8} \frac{cm^3}{g \sec^2}$$
 
$$pc = 3.085 \times 10^{18} cm$$
 
$$M_{\odot} = 2 \times 10^{33} g$$

## The Stellar and Gas Kinematics of the LITTLE THINGS Dwarf Irregular Galaxy NGC 1569

Megan Johnson<sup>1,2,3,10</sup>, Deidre A. Hunter<sup>2,10</sup>, Se-Heon Oh<sup>4,5</sup>, Hong-Xin Zhang<sup>2,6</sup>, Bruce Elmegreen<sup>7</sup>, Elias Brinks<sup>8</sup>, Erik Tollerud<sup>9</sup>, Kimberly Herrmann<sup>2</sup>

#### ABSTRACT

In order to understand the formation and evolution of Magellanic-type dwarf irregular (dIm) galaxies, one needs to understand their three-dimensional structure. We present measurements of the stellar velocity dispersion in NGC 1569, a nearby post-starburst dIm galaxy. The stellar vertical velocity dispersion,  $\sigma_z$ , coupled with the maximum rotational velocity derived from H I observations,  $V_{\text{max}}$ , gives a measure of how kinematically hot the galaxy is, and, therefore, indicates its structure. We conclude that the stars in NGC 1569 are in a thick disk with a  $V_{\rm max}/\sigma_z$  $= 2.4 \pm 0.7$ . In addition to the structure, we analyze the ionized gas kinematics from O III observations along the morphological major axis. These data show evidence for outflow from the inner starburst region and a potential expanding shell near supermassive star cluster (SSC) A. When compared to the stellar kinematics, the velocity dispersion of the stars increase in the region of SSC A supporting the hypothesis of an expanding shell. The stellar kinematics closely follow the motion of the gas. Analysis of high resolution H I data clearly reveals the presence of an H I cloud that appears to be impacting the eastern edge of NGC 1569. Also, an ultra-dense H I cloud can be seen extending to the west of the impacting H I cloud. This dense cloud is likely the remains of a dense H I bridge that extended through what is now the central starburst area. The impacting H I cloud was the catalyst for the starburst, thus turning the dense gas into stars over a short timescale,  $\sim 1$  Gyr. We performed a careful study of the spectral energy distribution using infrared, optical, and ultraviolet photometry producing a state-of-the-art mass model for the stellar disk. This mass modeling shows that stars dominate the gravitational potential in the inner 1 kpc. The dynamical mass of NGC 1569, derived from  $V_{\text{max}}$ , shows that the disk may be dark matter deficient in the inner region, although, when compared to the expected virial mass determined from halo abundance matching techniques, the dark matter profile seems to agree with the observed mass profile at a radius of 2.2 kpc.

Subject headings: galaxies: individual (NGC 1569) — galaxies: dwarf galaxies — galaxies: starburst — galaxies: kinematics — galaxies: spectroscopy

<sup>&</sup>lt;sup>1</sup>National Radio Astronomy Observatory, PO Box 2, Green Bank, WV 24944; mjohnson@nrao.edu

<sup>&</sup>lt;sup>2</sup>Lowell Observatory, 1400 West Mars Hill Road, Flagstaff, AZ 86001; dah@lowell.edu, hxzhang@lowell.edu, herrmann@lowell.edu

<sup>&</sup>lt;sup>3</sup>Georgia State University, 1 Park Place South SE, Suite 700, Atlanta, GA 30303-2911

<sup>&</sup>lt;sup>4</sup>International Centre for Radio Astronomy Research (ICRAR), University of Western Australia, 35 Stirling Highway, Crawley, WA 6009, Australia; seheon.oh@uwa.edu.au

<sup>&</sup>lt;sup>5</sup>ARC Centre of Excellence for All-sky Astrophysics

<sup>(</sup>CAASTRO)

 $<sup>^6 \</sup>mathrm{Purple}$  Mountain Observatory, Chinese Academy of Sciences

<sup>&</sup>lt;sup>7</sup>IBM T.J. Watson Research Center, 1101 Kitchawan Road, Yorktown Hts., NY 10598; bge@us.ibm.com

<sup>&</sup>lt;sup>8</sup>Centre for Astrophysics Research, University of Hertfordshire, College Lane, Hatfield, AL10 9AB, UK; E.Brinks@herts.ac.uk

<sup>&</sup>lt;sup>9</sup>Center For Cosmology, Department of Physics and Astronomy, 4129 Frederick Reines Hall, University of California, Irvine; etolleru@uci.edu

<sup>&</sup>lt;sup>10</sup>Visiting Astronomer, Kitt Peak National Observatory

complicated kinematics, and we will present evidence here and in a forthcoming paper (Johnson, in prep) of an interaction or a past merger that has created the dIm galaxy we observe today.

This work is part of a large collaborative effort called Local Irregulars That Trace Luminosity Extremes, The H I Nearby Galaxy Survey (LITTLE THINGS; Hunter & Elmegreen 2012). One of the goals of the LITTLE THINGS survey is to understand how dIm galaxies form stars. LITTLE THINGS is a multi-wavelength study of 37 dIm and 4 Blue Compact Dwarf (BCD) galaxies. LIT-TLE THINGS was granted close to 376 hours in 2007 and 2008 on the NRAO<sup>1</sup> Very Large Array (VLA) in the B-, C-, and D-array configurations in order to obtain deep H I maps for 21 galaxies. The other 20 galaxies are from the VLA archives. In addition to the H I data, LITTLE THINGS has extensive  $H\alpha$  and optical photometry for each dIm galaxy from previous studies (Hunter & Elmegreen 2004, 2006) and has also collected GALEX ultraviolet images for most and near- and mid-infrared data (ground based JHK and Spitzer) for a subsample.

Our paper is structured as follows: Section 2 describes the observations and data reductions for the optical spectroscopy and the H I data used in this study. Section 3 discusses our data analysis; Section 4 outlines our observational results; Section 5 describes our mass modeling; Section 6 is our discussion; Section 7 is a summary of our results.

#### 2. Data

#### 2.1. Stellar Optical Spectroscopy

#### 2.1.1. Observations

We observed NGC 1569 with the Kitt Peak National Observatory (KPNO<sup>2</sup>) Mayall 4-meter telescope with the Echelle spectrograph for three nights in February 2008 and five nights in November 2008. The sky conditions for the February

2008 observing run were moderate with only a few cirrus clouds interfering sporadically throughout the run. The moon was in a waning crescent phase and was separated by more than 180° from NGC 1569. The weather conditions for the November 2008 observing run were superb with nearly photometric conditions throughout the five nights, however, the moon passed through third quarter during the second night of our run but was separated from NGC 1569 by more than 60°.

Table 2 lists the observation log. In order to place the slit, we identified the center of the galaxy and position angle (PA) of the major axis from iso-intensity contours on our V-band image. We observed at four PAs, all centered on the morphological center of the galaxy: the major axis (PA = 121°), the minor axis (PA = 31°) and  $\pm 45^\circ$  from the major axis. Figure 2 shows the  $HST^6$  V-band, O III  $\lambda 5007 \text{Å}$ , H $\beta$  and H $\alpha$  filter composite image of NGC 1569 taken with the Advanced Camera for Surveys and the Wide Field Planetary Camera 2 instruments (bottom panel) with the slit positions superimposed.

We converted the Echelle into a two-dimensional. - long-slit spectrograph by replacing the crossdisperser with a mirror flat. This permitted the isolation of a single order and produced a 3' long slit. In order to maximize throughput, while maintaining high spectral resolution, we opened the slit to a width of 2".5. For the stellar kinematic data, we targeted the prominent Mg Ib stellar absorption features at wavelengths 5183.6 Å, 5172.7 Å, and 5167.3 Å, by isolating order 10 for the 316-63° Echelle using the post-slit filter KP 1433. This filter has a central wavelength of 5204 Å and a full-width half-maximum (FWHM) of 276 Å. The free spectral range of the Echelle was 517 Å centered at 5170 Å, but, for the Tektronics 2048 x 2048 CCD that we used, only 286 Å fit across the chip. We used the "fast UV" camera along with pre-slit filter GG 495. The prominent Mg Ib stellar absorption features were easily detected. There are no telluric features in the spectral region we observed.

For our spectral range, this setup provided a

<sup>&</sup>lt;sup>1</sup>National Radio Astronomy Observatory (NRAO) is a facility of the National Science Foundation operated under cooperative agreement by Associated Universities, Inc.

<sup>&</sup>lt;sup>2</sup>The Kitt Peak National Observatory is operated by the National Optical Astronomy Observatory (NOAO), which is operated by the Association of Universities for Research in Astronomy (AURA) under cooperative agreement with the National Science Foundation.

<sup>&</sup>lt;sup>3</sup> Hubble Space Telescope (HST), is operated by NASA and ESA at the Space Telescope Science Institute (STScI). STScI is operated by the Association of Universities for Research in Astronomy, Inc., under NASA contract NAS

before and after sky subtraction.

#### 2.2. Ionized Gas Optical Spectroscopy

#### 2.2.1. Observations and Data Reductions

A different post-slit filter (KP 1547) was used for the ionized gas, but otherwise, the telescope setup was unchanged. The KP 1547 filter has a central wavelength of about 5015 Å and a FWHM of 27 Å, and was used for targeting the O III  $\lambda$ 5007 Å emission feature. We observed both the major and minor axes. We took dome flats, twilight flats, and stepped one radial velocity standard star along the slit spatially to correct for the slit distortion and to find the center of the slit in the same fashion as for the other filter, described previously.

Additionally, we took Th-Ar comparison lamp exposures after all object images for accurate wavelength calibration. We observed three galaxy and three sky positions for the major axis PA, and three galaxy positions for the minor axis. However, due to threatening clouds during the course of the night, we were only able to observe one sky image for the minor axis. The sky image was scaled to compensate for the large difference in exposure time. Despite the difficulties, the brightness of the O III emission line made it possible to obtain high signal-to-noise emission line spectra. We followed the same data reduction procedure as for the stellar spectral data. Figure 4 shows the fully reduced, two-dimensional, co-added, O III  $\lambda 5007$  Å emission spectrum for the major and minor axes of NGC 1569.

#### 2.3. H I Data

The LITTLE THINGS project retrieved the calibrated H I line uv-data from THINGS but improved upon the quality of the THINGS data products by applying a multi-scale cleaning algorithm implemented in the AIPS task IMAGR (see, e.g., Cornwell 2008; Rich et al. 2008; Greisen et al. 2009). Instead of approximating all structures as a sum of point sources, this algorithm iteratively fits Gaussians to four angular scales of 135", 45", 15", and 0", respectively. The multi-scale cleaning algorithm produces a single data cube in which all observed angular frequencies are properly represented and with near uniform (Gaussian) noise statistics, which is a great advantage over standard cleaning methods. A beam size of 7"71 x

7".04 (with a position angle of 16.5) and a spectral resolution of 2.6 km s<sup>-1</sup> were achieved.

In order to separate noise from real galaxy emission, we used the Natural-weighted cube and smoothed it to a  $25''\times25''$  (CONVL) beam. We blanked this smoothed cube twice, first for all pixels below  $2.5~\sigma$  of the rms of the smoothed cube (Blank), and then again by hand for any additional emission that was clearly noise. This final, blanked cube became the master for the cubes with smaller beam sizes and was used as a conditional transfer. For a comprehensive review of our mapping procedure, please see Hunter et al. (submitted).

The half-power beam width (HPBW) of the primary beam is 32', but the largest angular scale of emission that is expected to be recovered by the interferometer is  $\sim 15'$ , which is determined by the D-array. Any smooth structure larger than  $\sim 15'$  will be invisible to the interferometer. This was useful in removing foreground Milky Way HI emission, which has velocities that partly overlap with some of the velocities encountered in NGC 1569. In essence, the interferometer is blind for emission from the Milky Way, and will only register its small-scale structure, which is still considerably more extended than that of NGC 1569. The multi-scale cleaning algorithm was able to model this Milky Way emission sufficiently well so emission from NGC 1569 could be isolated from the rest using the blanking method described above. A more in depth discussion of Milky Way confusion with NGC 1569 is discussed in our upcoming paper describing the map made with the Green Bank Telescope (GBT) (Johnson, in preparation, hereafter Paper II).

Figure 5 shows the LITTLE THINGS integrated flux map. This image shows tenuous emission to the south and northeast of the galaxy that are imaged for the first time. Although faint, this low-level, extended emission was confirmed in follow up observations with the Robert C. Byrd Green Bank Telescope (GBT) and will be discussed in Paper II.

fitting template. Also, we observed no trend between stellar spectral types or classes when determining a "good-fitting" versus an "ill-fitting" template in the CCM; S/N dominated the quality of the fit.

To determine the intrinsic velocity dispersions of the stars,  $\sigma_{\rm obs}$ , in NGC 1569 as a function of radius, we employ the definition of a Gaussian and correct for instrumental broadening using the following equation:

$$\sigma_{\rm obs} = \frac{\sqrt{\rm FWHM_{obs}}^2 - \rm FWHM_{\rm instr}}^2}{2.35} \qquad (1)$$

We determine the inherent, average instrumental full-width half-maximum, FWHM $_{\rm instr}=35$  km s<sup>-1</sup>, by cross-correlating the template stars from a single night with each other. The intrinsic broadening of a single star should be unresolved, so the FWHM $_{\rm instr}$  of the cross-correlation of the template stars with each other represents the instrumental signature. Although the spectral types and classes of the radial velocity standard stars span a range, our usable wavelength region is only  $\sim$  150 Å, thus cross-correlations of the stars between differing spectral types did not create variations in the resulting FWHM $_{\rm instr}$  or FWHM $_{\rm obs}$  above their respective standard deviations.

#### 3.2. Ionized Gas Optical Spectroscopy

#### 3.2.1. Extracting One-Dimensional Spectra

Due to the starburst nature of NGC 1569, many star forming regions lie throughout the observable disk and create bright O III features seen along the cross-dispersion direction of these spectra. Figure 4 shows the two-dimensional spectra of the O III  $\lambda 5007$  Å emission feature observed in NGC 1569 along the major axis, top panel, and minor axis, bottom panel. Because the emission features are so bright, we are able to extract a single spectrum from each cross-dispersion row, giving an angular resolution of 1".09 per pixel (17.7 pc). Also, we achieve a velocity resolution of ~27 km s<sup>-1</sup> as measured from a comparison lamp emission line at  $\lambda = 5014$  Å with a FWHM of 0.46 Å. This corresponds to a velocity dispersion,  $\sigma$ , of ~12 km s<sup>-1</sup>.

#### 3.2.2. Multiple Gaussian Decomposition

Figure 8 shows an example of a single extracted spectrum of the O III  $\lambda5007$  Å emission feature taken from the major axis. It is evident that there are three distinct, bright peaks over a total width of 4.1 Å, or, ~176 km s<sup>-1</sup>. We disentangled these blended features with multiple Gaussian components (SPLOT). The three velocities obtained for the brightest three peaks in Figure 8 are -133.9, -84.2, and -31.5 km s<sup>-1</sup> spanning a range of over 100 km s<sup>-1</sup> at a distance of -13".2 from the center of the galaxy along the major axis. This fitting procedure was repeated for each spectrum extracted along the cross-dispersion axis.

# 3.3. Extracting the H I Bulk Velocity Field

#### 3.3.1. Tilted Ring Models

We use the newly imaged LITTLE THINGS H I data to determine the maximum rotation,  $V_{\rm max}$ , of the H I gas for NGC 1569. One common method of constructing rotation curves of disk galaxies from high-resolution H I data is the tilted ring model (Begeman 1989). The first step in applying this model is to create a two-dimensional velocity field out of a three-dimensional H I data cube. Then, from the extracted velocity map, a series of ring parameters are determined by independently fit-

pendently to each of the pre-determined rings in succession.

To determine the rotation curve of NGC 1569 we use the GIPSY<sup>5</sup> task ROTCUR, which applies the tilted ring model. We input the bulk velocity

<sup>&</sup>lt;sup>5</sup>The Groningen Image Processing SYstem (GIPSY) has been developed by the Kapteyn Astronomical Institute.

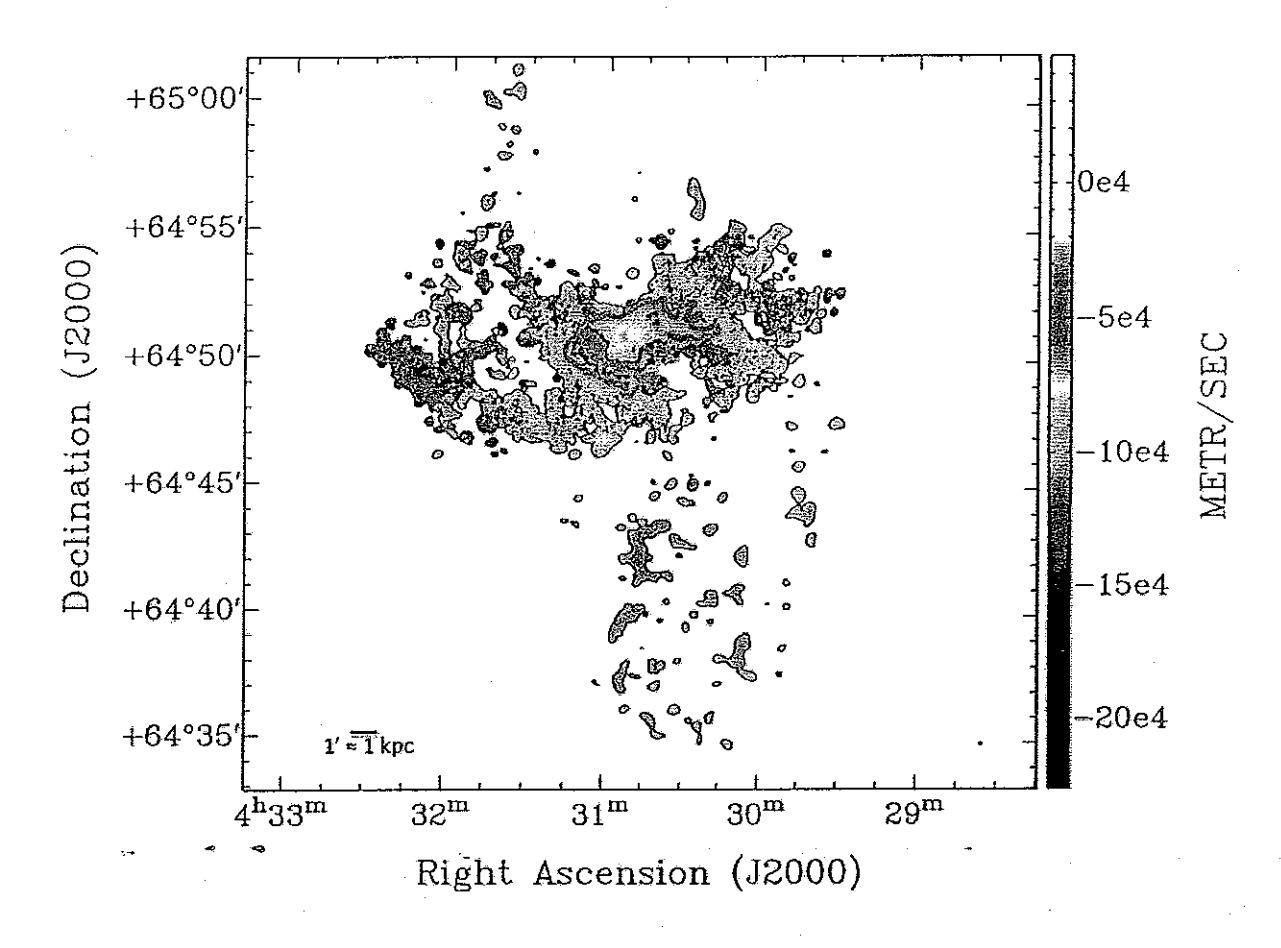


Fig. 9.— Intensity-weighted H I velocity field of NGC 1569. The red outline identifies the region over which the bulk motion extraction procedure was performed. The black line marks a ~1 kpc distance scale. The tiny dot in the lower right corner near (04:29:35, +64:35:00) shows the resolution.

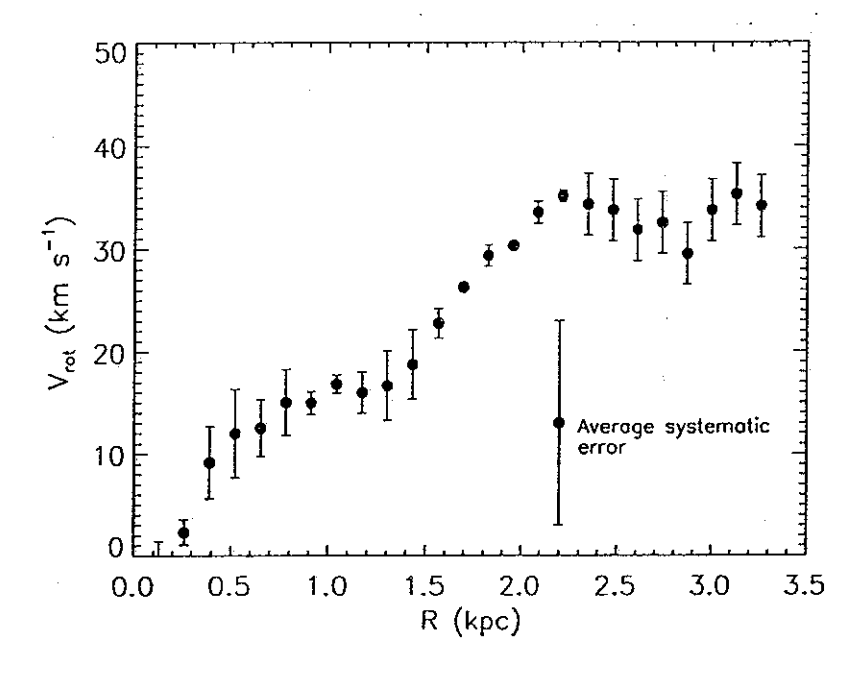


Fig. 15.— Measured rotation curve of the H I gas determined from the bulk motion map using a tilted ring model. A  $V_{\rm rot}$  of 33 km s<sup>-1</sup> is determined from averaging over the region where the curve is flat from  $\sim 2.0$  - 3.2 kpc. The errors on the rotation curve points are the standard deviations calculated by assuming a solid body rotation out to 2.2 kpc. The average systematic error, determined from all observational and computational uncertainty, is shown for reference.



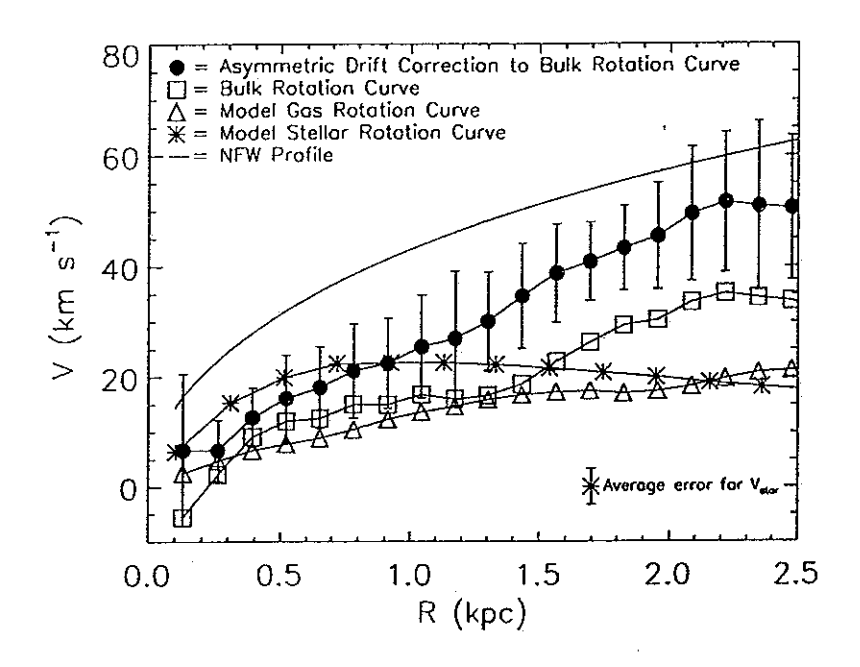


Fig. 17.— Mass modeling of both the stars (asterisks) and the gas (triangles) along with the observed bulk rotation curve (boxes) and the asymmetric drift corrected rotation curve (filled circles). The NFW profile (solid line) is also shown. The average uncertainty for the model stellar rotation are shown in the lower right corner for comparison to the asymmetric drift corrected rotation curve. Within the uncertainties, the stellar mass dominates the entire rotation curve out to 1 kpc, half of the observable stellar and gas disks.



Table 1
Global Parameters for NGC 1569

Global Parameters for NGC 1569		
Parameter	Value	Ref
Other names	UGC 03056, ARP 210,	1
	VII Zw 016	
D (Mpc)	$3.36 \pm 0.20$	. 2
Mv	-18.2	3
$\mu_{25}$ (mag arcsec <sup>-2</sup> )	22.3	5
Galaxy diameter to 25 mag arcsec <sup>-2</sup> in $B$ , $D_{25}$ (arcmin)	3.6	. 3
V-band disk scale length, $R_D$ (arcmin)	$0.39 \pm 0.02$	3
Center (R.A., decl.) (J2000)	(04:30:49.8, +64:50:51)	3
Minor-to-major axis ratio, b/a	0.55	3
$L_{\text{H}\alpha} \text{ (erg s}^{-1})$	$5.7 \times 10^{40}$	4
Star formation rate (SFR <sub>D</sub> ) ( $M_{\odot}$ yr <sup>-1</sup> kpc <sup>-2</sup> )	1.3	4
H <sub>2</sub> mass (M <sub>☉</sub> )	$5 \times 10^7$	6
Stellar parameters determined	from this work	
$V_{\text{sys}} (\text{km s}^{-1})$	-82 ± 7	
Major axis P.A. (deg)	121	
Inclination from de-projection, iopt (deg)	$60 \pm 10$	
Average velocity dispersion, $(\sigma_z)$ (km s <sup>-1</sup> )	21 ± 4	
Velocity dispersion near SSC A, σ <sub>z</sub> (km s <sup>-1</sup> )	33 ± 9	
Total stellar mass $(M_{\odot})$	$2.8 \times 10^{8}$	
Optical scale length, h (kpc)	1.54	
Optical scale height, z <sub>o</sub> (kpc)	0.31	
H1 parameters determined f	rom this work	
$V_{\rm sys}$ (km s <sup>-1</sup> ),	-85	
Major axis P.A. (deg)	122	
Inclination from tilted ring model, iH1 (deg)	69 ± 7	
Kinematic center $(X_{pos}, Y_{pos})$ (R.A., decl.)	(04:30:46.125, +64:51:10.25)	
$V_{\rm rot}$ (km s <sup>-1</sup> )	$33 \pm 10$	
$V_{\text{max}}$ (km s <sup>-1</sup> )	50 ± 10	
Average velocity dispersion, $(\sigma_{\rm H_1})$ (km s <sup>-1</sup> )	10	
Total gas mass $(M_{\odot})$	$2.3 \times 10^8$	
$M_{ m dyn} (M_{ m O})$		
$M_{\mathrm{DM}}\left(M_{\mathrm{\odot}}\right)$		
$M_{\mathrm{vir}}(M_{\odot})$		
R <sub>vir</sub> (kpc)		
$V_{\rm max}/\sigma_{\rm z}$	2.4 ± 0.7	

References. (1) NASA Extragalactic Database; (2) Grocholski et al. 2008; (3) Hunter & Elmegreen 2006; (4) Hunter & Elmegreen 2004; (5) de Vaucouleurs et al. 1991; (6) Israel 1988.